Supplementary Information

Coenzyme Corona Formation on Carbon Nanotubes Leads to Disruption of the Redox Balance in Metabolic Reactions

Atsushi Hirano,[†],* Tomoshi Kameda,[‡] Momoyo Wada,[†] Takeshi Tanaka,[†] Hiromichi Kataura[†]

[†] Nanomaterials Research Institute, National Institute of Advanced Industrial Science and Technology (AIST),
Tsukuba, Ibaraki 305-8565, Japan

[‡] Artificial Intelligence Research Center, National Institute of Advanced Industrial Science and Technology (AIST), Koto, Tokyo 135-0064, Japan

Corresponding author: hirano-a@aist.go.jp (A.H.)

Contents

1. Results

References

1 A. Hirano, Y. Maeda, X. Yuan, R. Ueki, Y. Miyazawa, J. Fujita, T. Akasaka and K. Shiraki, *Chem. - A Eur. J.*, 2010, **16**, 12221–12228.

2 A. Hirano, Y. Maeda, T. Akasaka and K. Shiraki, *Chem. - A Eur. J.*, 2009, **15**, 9905–9910.

3 V. Lvovich and A. Scheeline, *Arch. Biochem. Biophys.*, 1995, **320**, 1–13.

4 J. D. Yang, B. L. Chen and X. Q. Zhu, *J. Phys. Chem. B*, 2018, **122**, 6868–6898.

5 A. Hirano, M. Wada, T. Tanaka and H. Kataura, *ACS Nano*, 2019, **13**, 1805–1816.

6 A. Hirano, T. Kameda, M. Wada, T. Tanaka and H. Kataura, *J. Phys. Chem. Lett.*, 2017, **8**, 5216–5221.

1.1 Observation of the dispersibility of NADH-Dispersed CNTs in the Presence of NaCl or HCl/NaOH.

The 1266-nm absorbance of NADH-dispersed CNTs in the presence of NaCl or HCl/NaOH was measured after the centrifugation at 16,100×g for 1 min, where the samples were prepared by mixing a 200-µL aliquot of the NADH-dispersed CNTs with a 50-µL aliquot of NaCl or HCl/NaOH solutions at different concentrations. A decrease in absorbance indicates a decrease in CNT dispersibility. The decrease in absorbance in the presence of NaCl and at basic pH values is ascribable to the electrostatic screening of NADH adsorbed on the CNTs by the sodium ions (Figure S1);[1] note that the solutions at pH 10 and pH 11.2 contains approximately 40 mM and 400 mM sodium ions. The decrease in absorbance at acidic pH values is ascribable to the reduction of electrostatic repulsion,[2] because of protonation of the NADH phosphate groups.

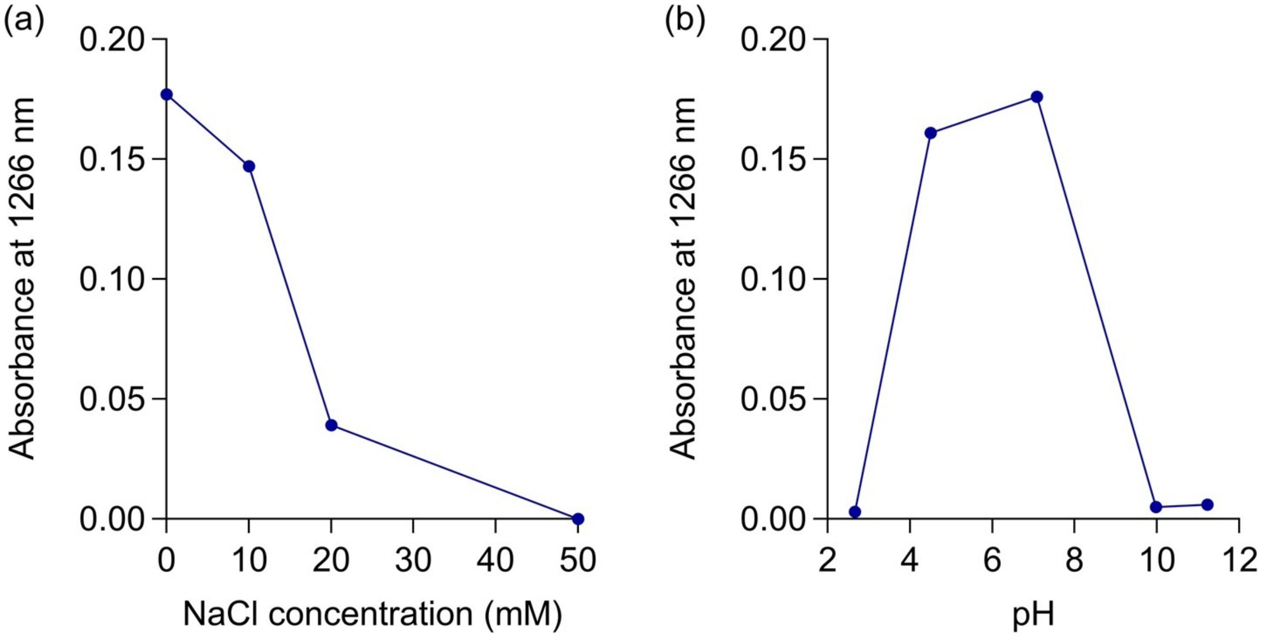

Figure S1. Dispersibility of the NADH-dispersed CNTs. (a,b) Absorbance of the NADH-dispersed CNTs at 1266 nm was measured at different concentrations of NaCl (a) or at different pH values (b).

1.2 Observation of the Redox State of CNTs in the Presence of Iron Ions. The absorbance of SDS-dispersed CNTs at 1266 nm was sufficiently high in a 50 µM $FeCl_3$ solution and sufficiently low in a 50 µM $FeCl_2$ solution (Figure S2). Accordingly, the absorbance values in the presence of 50 µM $FeCl_3$ and $FeCl_2$ can be regarded as those of completely oxidized and reduced CNTs, respectively.

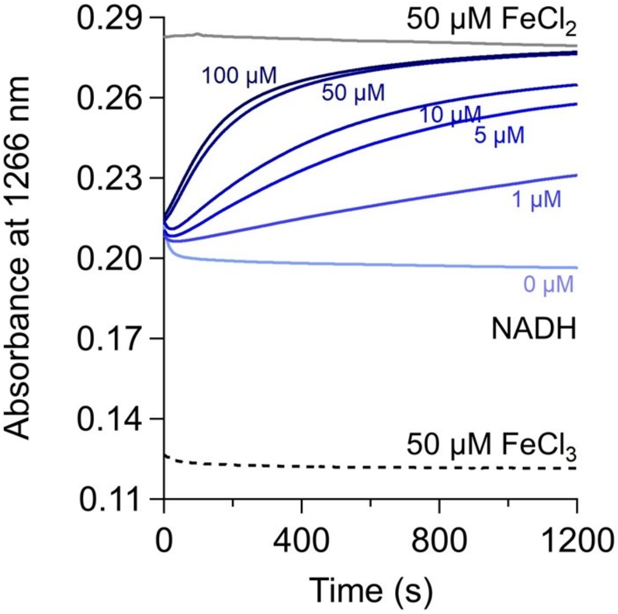

Figure S2. Time courses of absorbance of the CNTs at 1266 nm in the presence of 50 µM $FeCl_3$ or $FeCl_2$. The time courses at different concentrations of NADH are also shown as references.

1.3 A Suggested Reaction Model for Numerical Simulations. Numerical simulations were performed on the basis of Equations 1–3 as described in Scheme S1. Equation 1 assumes that the complexation of two NADH molecules with Fe^{3+} is a rate-limiting step.[3] The resulting NADH radical ($NADH^{+\cdot}$) is ultimately transformed to NAD^+ by the contribution of water;[4] this reaction should be slow ($k = 0.02$ (M^{-1} s^{-1})) (Figure S3). Equation 2 assumes a reversible reaction of iron ions with CNTs, as reported by a previous paper, which has a one-electron transfer process. Equation 3 assumes that two electrons are transferred from one NADH molecule to a CNT. On the basis of the reaction equations, reaction rate expressions were established as described in Equations 4–9 in Scheme S1. The rate constants k_0 and k_3 were experimentally determined in the present study (Figure 4), whereas the rate constants k_1 and k_2 were obtained from a previous work.[5]

Scheme S1. Assumed elementary reaction equations and reaction rate expressions. The parameter *k* is the reaction rate constant. The combination of Equations 1 and 2 corresponds to the indirect (transition metal-mediated) redox reaction between NADH and CNTs mediated by iron ions, while Equation 3 corresponds to the direct redox reaction between NADH and CNTs (Figure 5). Equations 4–9 are differential rate equations that are established on the basis of Equations 1–3. These equations were used for the numerical simulations of the redox reactions with a time difference (Δ*t*) of 0.5 s.

$$2\mathrm{NADH} + \mathrm{Fe}^{3+} \xrightarrow{k_0} 2\mathrm{NADH}\cdot\mathrm{Fe}^{3+} \rightarrow \mathrm{NADH} + \mathrm{NADH}^{+\cdot} + \mathrm{Fe}^{2+} \tag{1}$$

$$\mathrm{Fe}^{3+} + \mathrm{CNT} \underset{k_2}{\overset{k_1}{\rightleftarrows}} \mathrm{Fe}^{2+} + \mathrm{CNT}^{+} \tag{2}$$

$$\frac{1}{2}\mathrm{NADH} + \mathrm{CNT} \xrightarrow{k_3} \frac{1}{2}\mathrm{NAD}^{+} + \mathrm{CNT}^{+} + \frac{1}{2}\mathrm{H}^{+} \tag{3}$$

$$\frac{d[\mathrm{NADH}]}{dt} = -k_0[\mathrm{NADH}]^2[\mathrm{Fe}^{3+}] - k_3[\mathrm{NADH}]^{\frac{1}{2}}[\mathrm{CNT}^{+}] \tag{4}$$

$$\frac{d[\mathrm{Fe}^{3+}]}{dt} = -k_0[\mathrm{NADH}]^2[\mathrm{Fe}^{3+}] - k_1[\mathrm{Fe}^{3+}][\mathrm{CNT}] + k_2[\mathrm{Fe}^{2+}][\mathrm{CNT}^{+}] \tag{5}$$

$$\frac{d[\mathrm{CNT}]}{dt} = -k_1[\mathrm{Fe}^{3+}][\mathrm{CNT}] + k_2[\mathrm{Fe}^{2+}][\mathrm{CNT}^{+}] + 2k_3[\mathrm{NADH}]^{\frac{1}{2}}[\mathrm{CNT}^{+}] \tag{6}$$

$$\frac{d[\mathrm{NAD}^{+}]}{dt} = -\frac{d[\mathrm{NADH}]}{dt} \tag{7}$$

$$\frac{d[\mathrm{Fe}^{2+}]}{dt} = -\frac{d[\mathrm{Fe}^{3+}]}{dt} \tag{8}$$

$$\frac{d[\mathrm{CNT}^{+}]}{dt} = -\frac{d[\mathrm{CNT}]}{dt} \tag{9}$$

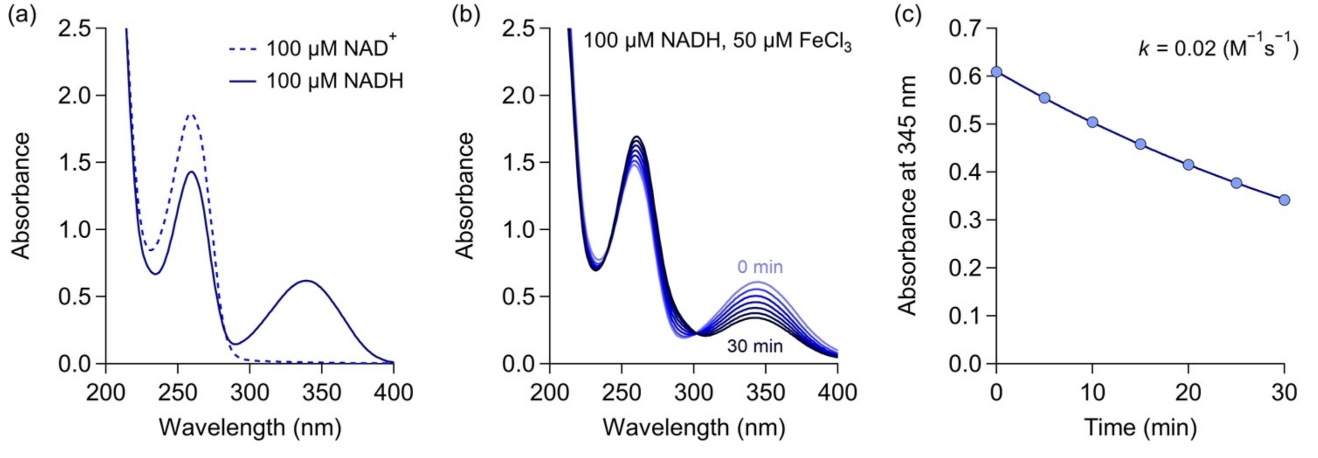

Figure S3. Chemical reactions of NADH with iron ions. (a) Absorption spectra of NAD at 100 μM. (b) Absorption spectra of NADH at 100 μM in the presence of 50 μM $\mathrm{FeCl_3}$ as a function of time. (c) A time course of absorbance at 345 nm in the spectra described in panel (b). The reaction involving the generation of $\mathrm{NAD^+}$ from $\mathrm{NADH^{+\cdot}}$ was regarded as pseudofirst-order because the reactant water is abundant.

1.4 Numerical Simulations for the Redox Reaction of CNTs in the Presence of NADH and Iron Ions. On the basis of the numerical simulations (Section 1.7), the NADH concentration monotonously decreases coincident with the generation of NAD$^+$ in the presence of $FeCl_3$ (Figure S4). The oxidation of NADH is more effectively facilitated at higher concentrations of $FeCl_3$.

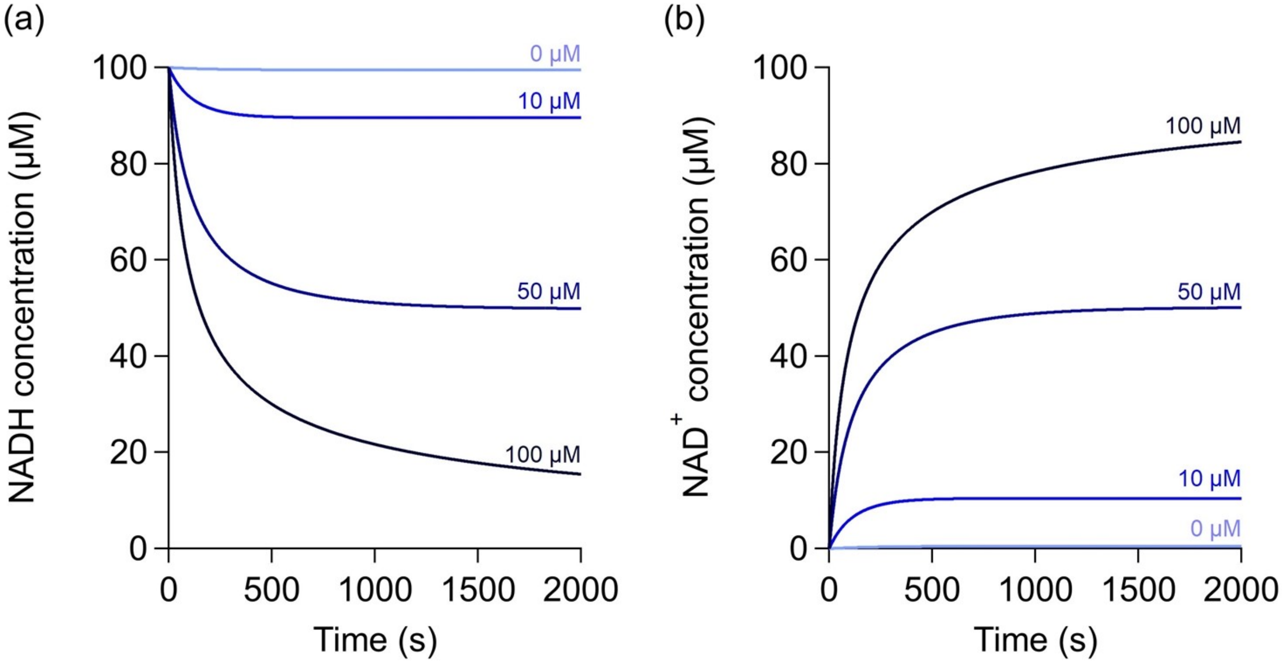

Figure S4. Numerical simulations for the redox reaction at different concentrations of $FeCl_3$ in the presence of 100 μM NADH. (a,b) Concentrations of NADH (a) and NAD$^+$ (b) were described as a function of time.

1.5 Observation of the Redox State of CNTs in the Presence of Copper and Zinc Ions. The absorbance of the CNTs at 1266 nm was increased by the addition of 100 μM NADH along with $CuCl_2$ or $ZnCl_2$ (Figure S5, left panel). The absorption peak intensities in the S_{11} band increased within 30 min of the addition of NADH and the metal ions (Figure S5, right panel).

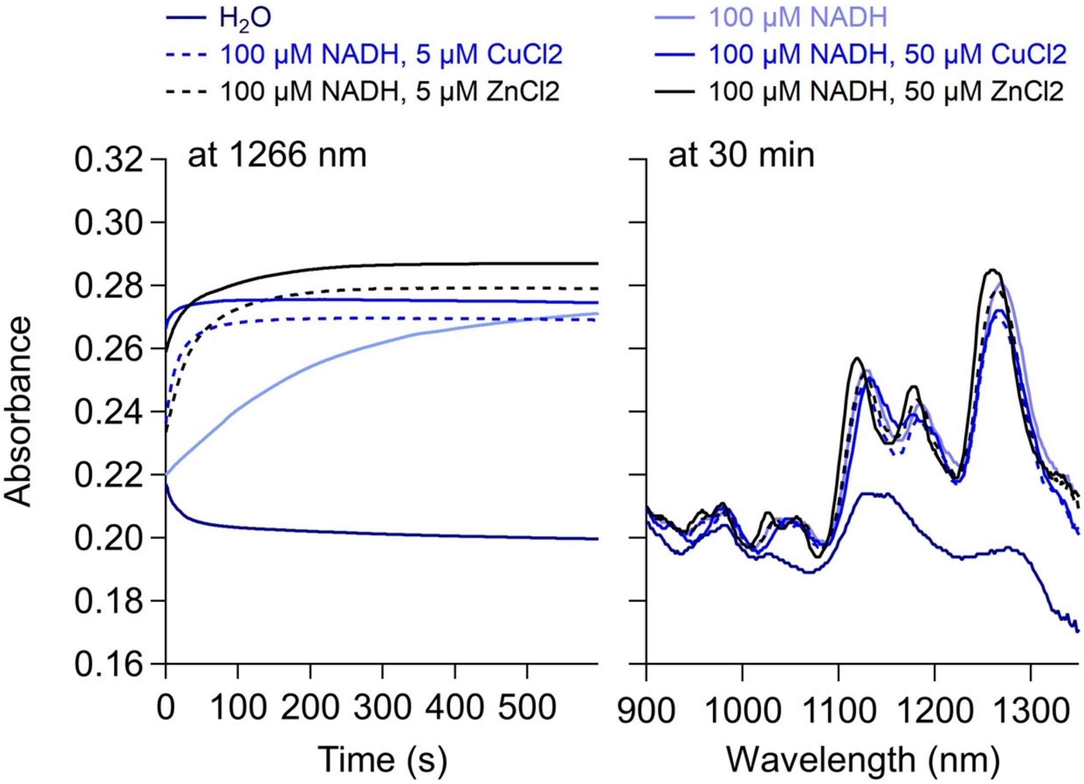

Figure S5. Redox reaction of NADH with CNTs in the presence of copper and zinc ions. Time courses of absorbance of the CNTs at 1266 nm (left panel) and absorption spectra of the CNTs at 30 min (right panel) after mixing with 0, 5 and 50 μM $CuCl_2$ or $ZnCl_2$ in the presence and absence of 100 μM NADH.

1.6 Determination of Chiral Indices of Metallic CNTs Using Raman Spectroscopy. The Raman spectrum of the SDS-dispersed CNTs was measured to identify the chiral indices of the CNTs contained in the sample. A peak was observed at approximately 277 cm^{-1}, which can be assigned to metallic CNTs, including (9,3) and (10,1) CNTs.[6]

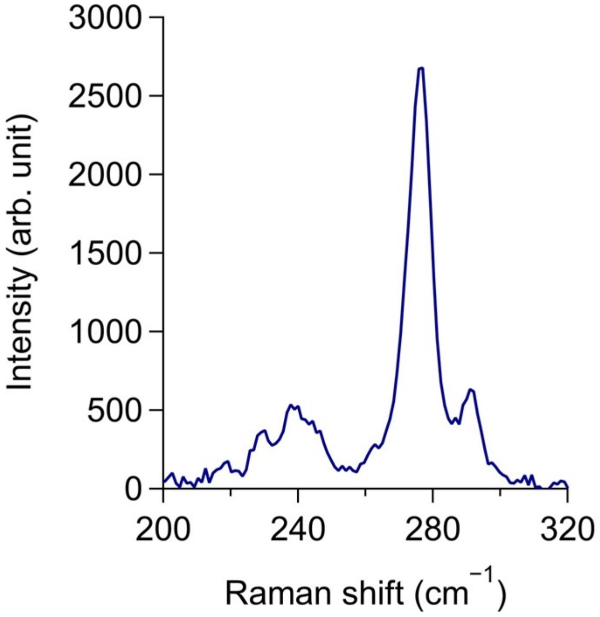

Figure S6. Radial breathing mode (RBM) Raman spectrum of the metallic CNTs excited at 532 nm. The peak at approximately 277 cm^{-1} can be assigned to (9,3) and (10,1) CNTs.

1.7 Redox Reaction of NAD and NAD Derivatives with Salmon Sperm DNA-Dispersed HiPco CNTs.

Absorption peak intensities in the S_{11} band of DNA-dispersed HiPco CNTs were increased within 30 min of the addition of NAD and NAD derivatives. This result suggests that the NAD molecules can access the solvent-exposed surfaces of the DNA-dispersed CNTs and can reduce them through electron transfer.

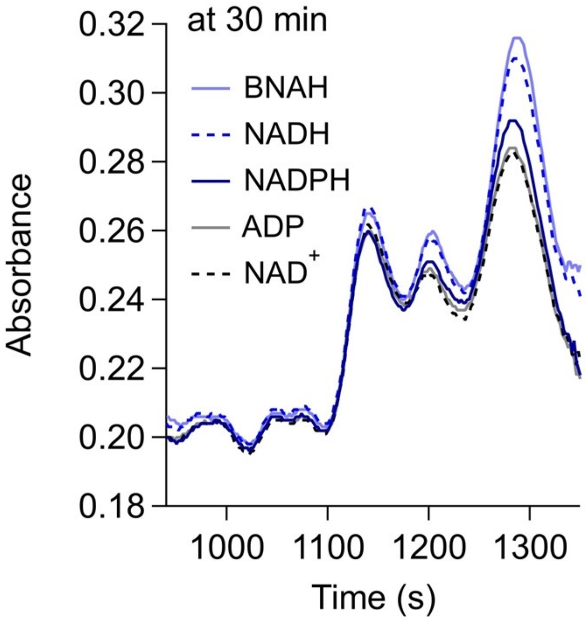

Figure S7. Redox reaction of NAD and NAD derivatives with the DNA-dispersed HiPco CNTs. Absorption spectra of the CNTs at 30 min after mixing with 100 μM NAD or NAD derivatives. The pH values were adjusted to 5–6.

1.8 Redox Reaction of NAD with Various DNA-Dispersed HiPco CNTs. The 1266-nm absorbance of the CNTs dispersed with various (human, bovine and salmon) DNA molecules was increased by the addition of 10 μM NADH (Figure S8, left panel). The absorption peak intensities in the S11 band increased within 30 min of the addition of NADH (Figure S8, right panel). Notably, in this experiment, the DNA-dispersed CNTs were prepared by the same procedure as described in Section 1.11, but with 0.2 mg/mL CNT, 0.02 wt % DNA, ultrasonication at a power density of ca. 16 W cm^{-2} and ultracentrifugation at 210,000×g for 10 min. The final compositions of the solutions were as follows: 0.05 mg/mL CNT, 0.02 wt % DNA and 0 or 10 μM NADH. The CNTs dispersed with human DNA are likely to be most susceptible to the redox reaction.

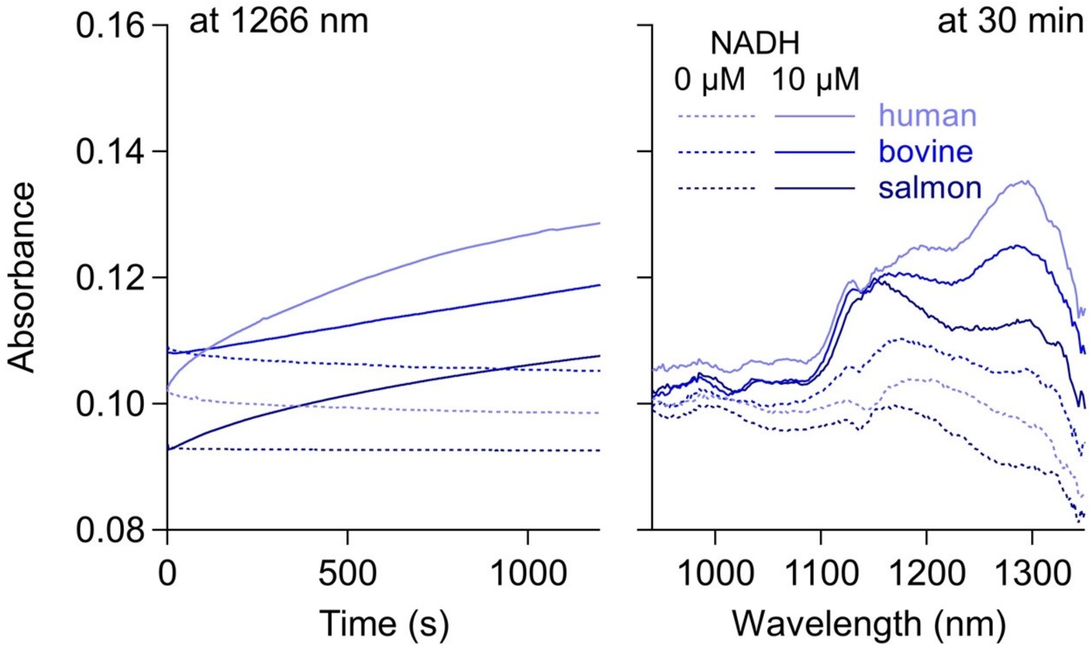

Figure S8. Time courses of absorbance of various DNA-dispersed HiPco CNTs at 1266 nm (left panel) and absorption spectra of them at 30 min (right panel) after mixing with 10 μM NADH.

1.9 Redox Reaction of NAD and NAD Derivatives with SDS-Dispersed CoMoCAT CNTs. CoMoCAT CNTs show an absorption peak at approximately 984 nm, which corresponds to the S_{11} band of (6,5) CNTs. The absorbance at 984 nm was increased by the addition of 100 μM BNAH, NADH and NADPH (Figure S9, left panel). An increase in peak intensity was also observed at approximately 570 nm, which corresponds to the S_{22} band of the (6,5) CNT (Figure S9, right panel). This result indicates electron transfer from the nicotinamide moiety of NADH to the S_{22} band of the CNT.

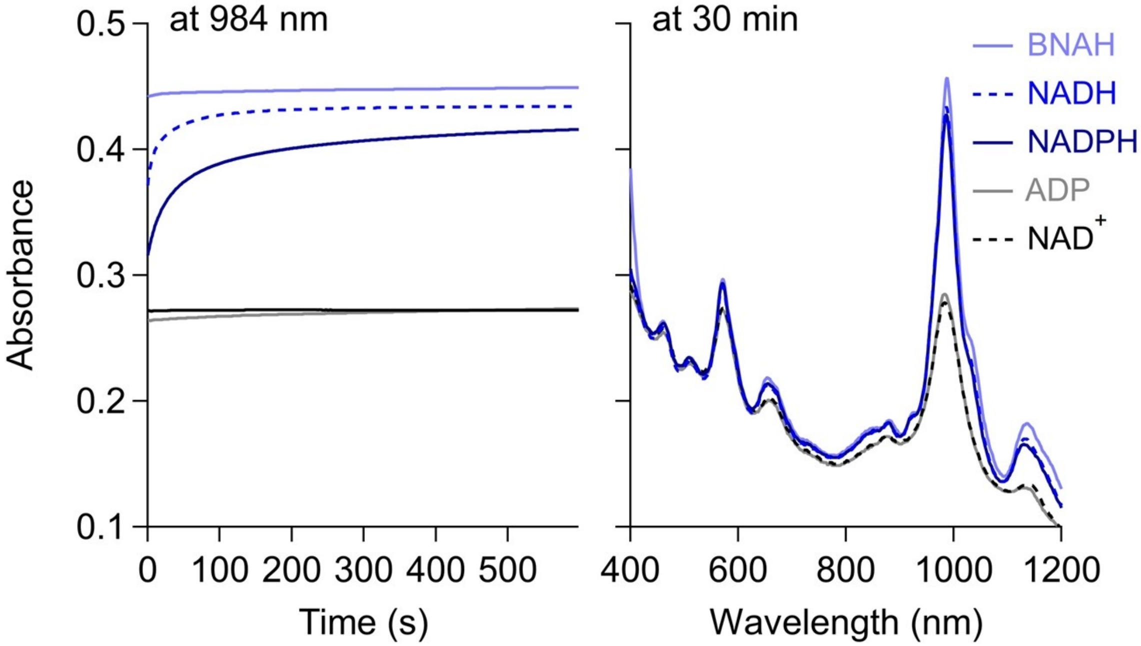

Figure S9. Time courses of absorbance of the SDS-dispersed CoMoCAT CNTs at 984 nm (left panel) and absorption spectra of them at 30 min (right panel) after mixing with 100 μM NAD or NAD derivatives.

1.10 Methods for the Preparation of Surfactant-Dispersed CNTs and the Examination of Enzymatic Reactions.

(a) Preparation of Surfactant-Dispersed CNTs for Absorption Spectroscopy

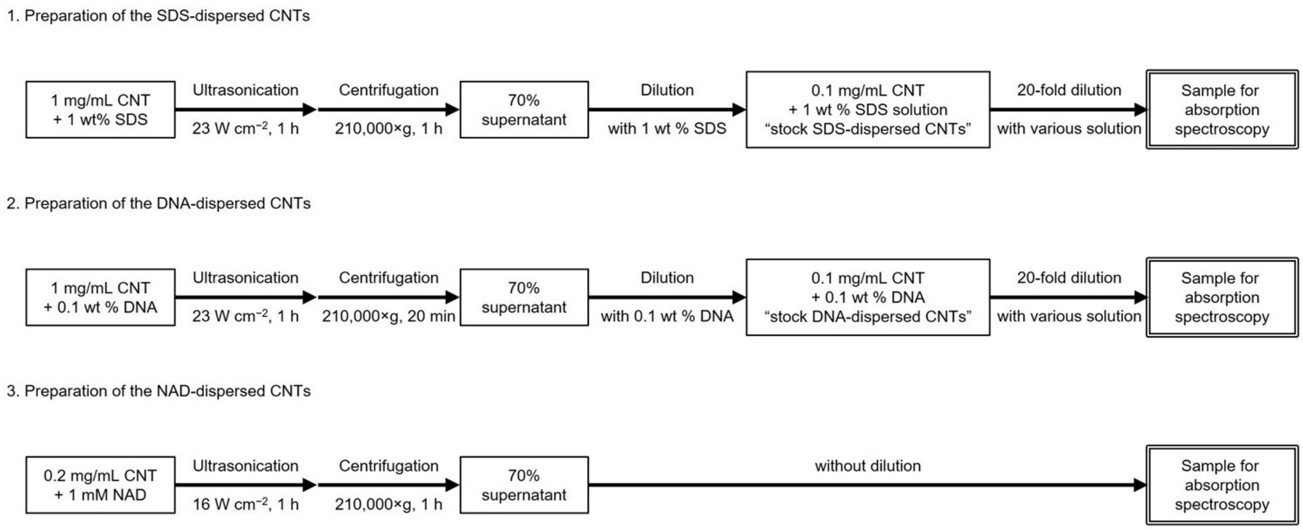

(b) Examination of Enzymatic Reactions of LDH in the Presence and Absence of CNTs

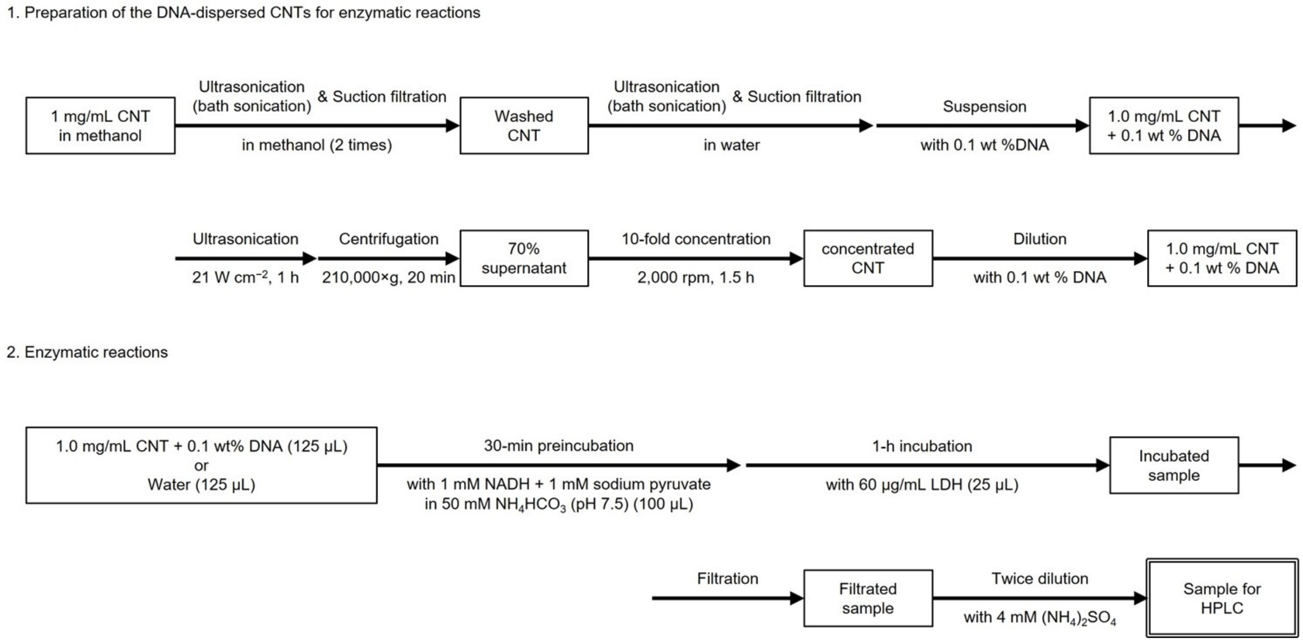

Figure S10. Flow chart of the sample preparation.

1.11 Information Regarding the Charge of BNAH Atoms.

The charge and atom type of the BNAH are described below in Tripos mol2 format.

```
@<TRIPOS>MOLECULE
BNA
   30   31    1    0    0
SMALL
No Charge or Current Charge


@<TRIPOS>ATOM
      1 C7          3.5400    1.4200    0.0000 ca         1 BNA     -0.153752
      2 C6          3.5070    1.5670   -1.3740 ca         1 BNA     -0.124898
      3 C3          2.3000    1.4750   -2.0540 ca         1 BNA     -0.218727
      4 H3          2.2830    1.5970   -3.1220 ha         1 BNA      0.140670
      5 H4          4.4140    1.7590   -1.9200 ha         1 BNA      0.142292
      6 H5          4.4720    1.4950    0.5310 ha         1 BNA      0.140562
      7 C5          2.3610    1.1810    0.6930 ca         1 BNA     -0.124898
      8 H2          2.3790    1.0700    1.7620 ha         1 BNA      0.142292
      9 C4          1.1610    1.0870    0.0130 ca         1 BNA     -0.218727
     10 H1          0.2490    0.9110    0.5570 ha         1 BNA      0.140670
     11 C1          1.1190    1.2310   -1.3700 ca         1 BNA      0.189560
     12 C2         -0.1860    1.0790   -2.1320 c3         1 BNA     -0.295842
     13 H6         -0.0480    1.4300   -3.1510 h1         1 BNA      0.111755
     14 H7         -0.4390    0.0270   -2.1990 h1         1 BNA      0.111755
     15 N1         -1.3090    1.7550   -1.5130 nh         1 BNA      0.380079
     16 C9         -2.5070    1.1190   -1.3180 c2         1 BNA     -0.250953
     17 H8         -2.4760    0.0540   -1.4500 h4         1 BNA      0.158658
     18 C8         -1.3010    3.1520   -1.4120 c2         1 BNA     -0.406088
     19 H9         -0.3620    3.6120   -1.6510 h4         1 BNA      0.210740
     20 C11        -2.3540    3.8530   -1.0360 c2         1 BNA     -0.155215
     21 H10        -2.2630    4.9220   -0.9720 ha         1 BNA      0.125240
     22 C12        -3.6740    3.2230   -0.6670 c3         1 BNA      0.110984
     23 H13        -4.4860    3.6870   -1.2240 hc         1 BNA      0.022598
     24 H14        -3.9070    3.4000    0.3800 hc         1 BNA      0.022598
     25 C10        -3.6310    1.7360   -0.9470 ce         1 BNA     -0.237840
     26 C13        -4.8720    0.9750   -0.6780 c          1 BNA      0.847652
     27 O1         -5.7430    1.4190    0.0210 o          1 BNA     -0.615965
     28 N2         -4.9840   -0.2790   -1.2390 n          1 BNA     -0.978561
     29 H11        -4.5910   -0.4200   -2.1410 hn         1 BNA      0.391681
     30 H12        -5.8910   -0.6800   -1.1210 hn         1 BNA      0.391681
@<TRIPOS>BOND
     1    2    1 ar
     2    3    2 ar
     3    4    3 1
     4    5    2 1
     5    6    1 1
     6    7    1 ar
     7    8    7 1
     8    9    7 ar
     9   10    9 1
    10   11    9 ar
    11   12   11 1
    12   13   12 1
    13   14   12 1
    14   15   12 1
    15   16   15 1
    16   17   16 1
    17   18   15 1
    18   19   18 1
    19   20   18 2
    20   21   20 1
    21   22   20 1
    22   23   22 1
    23   24   22 1
    24   25   22 1
    25   26   25 1
    26   27   26 2
    27   28   26 1
    28   29   28 1
    29   30   28 1
    30   11    3 ar
    31   25   16 2
@<TRIPOS>SUBSTRUCTURE
     1 BNA         1 TEMP              0 ****  ****    0 ROOT
```